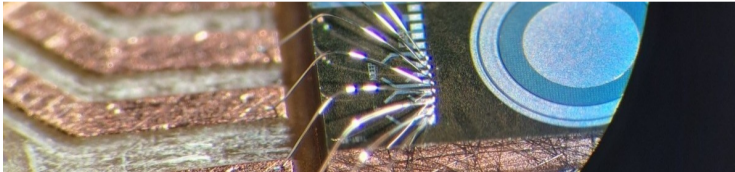


# Annealing effects on highly n-doped layers in Resistive AC-coupled Silicon Detectors

4th DRD3 week on Solid State Detectors RD

**Aurora Losana**<sup>1,2</sup>, Brendan Regnery<sup>1</sup>, Roberta Arcidiacono<sup>3,4</sup>, Nicolo Cartiglia<sup>3</sup>, Matteo Centis Vignali<sup>7</sup>, Alexander Dierlamm<sup>1</sup>, Marco Ferrero<sup>3</sup>, Alessandro Fondacci<sup>7</sup>, Ling Leander Grimm<sup>1</sup>, Frank Hartmann<sup>1</sup>, Markus Klute<sup>1</sup>, Luca Menzio<sup>3</sup>, Francesco Moscatelli<sup>5,6</sup>

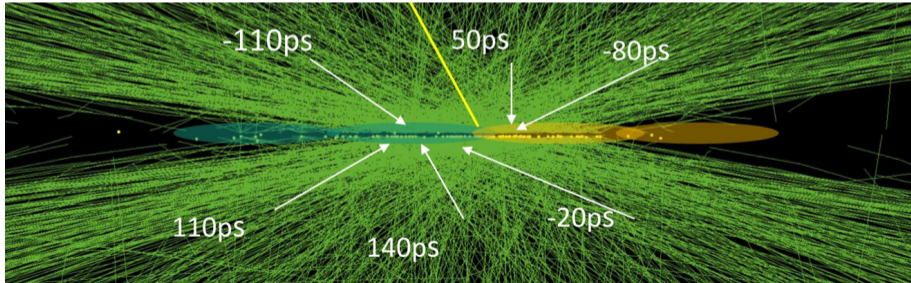
<sup>1</sup>KIT, <sup>2</sup>UNITO, <sup>3</sup>INFN Torino, <sup>4</sup>Università del Piemonte Orientale, <sup>5</sup>IOM-CNR Perugia, <sup>6</sup>INFN Perugia, <sup>7</sup>Fondazione Bruno Kessler



# Timing and 4D Tracking

Goal for the future:

- Increase the time resolution
  - Pile-up discrimination for hadron colliders
  - Time-of-Flight measurements for improved particle ID at lepton colliders.
- 4D Tracking
  - Reduce track finding combinatorics.



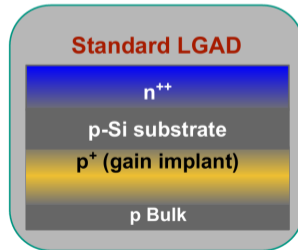
# Resistive Silicon Detector (RSD)

RSDs exploit the **time and amplitude differences** of the signals detected by **individual electrodes**.

50  $\mu\text{m}$  active thickness.

Signal shared between the readout electrodes.

} **Multiply the signal** to improve signal to noise ratio.



# Resistive Silicon Detector (RSD)

RSDs exploit the **time and amplitude differences** of the signals detected by **individual electrodes**.

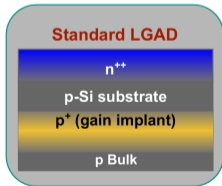
50  $\mu\text{m}$  active thickness.

Signal shared between the readout electrodes.

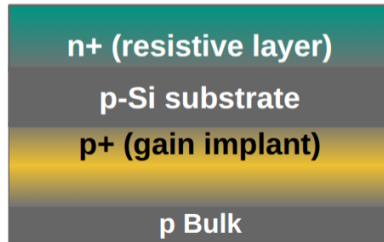
} **Multiply the signal** to improve signal to noise ratio.

The signal splits and propagates through the resistive layer, reaching the adjacent readout electrodes

} **n+ resistive layer** is functional to the signal sharing for improved spatial resolution.



+



# Resistive Silicon Detector (RSD)

RSDs exploit the **time and amplitude differences** of the signals detected by **individual electrodes**.

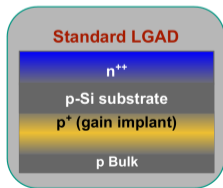
50  $\mu\text{m}$  active thickness.

Signal shared between the readout electrodes.

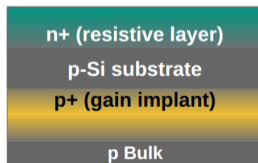
} **Multiply the signal** to improve signal to noise ratio.

The signal splits and propagates through the resistive layer, reaching the adjacent readout electrodes

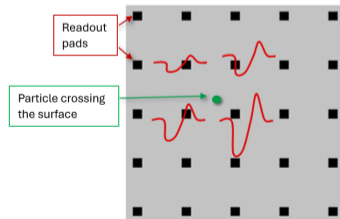
} **n+ resistive layer** is functional to the signal sharing for improved spatial resolution.



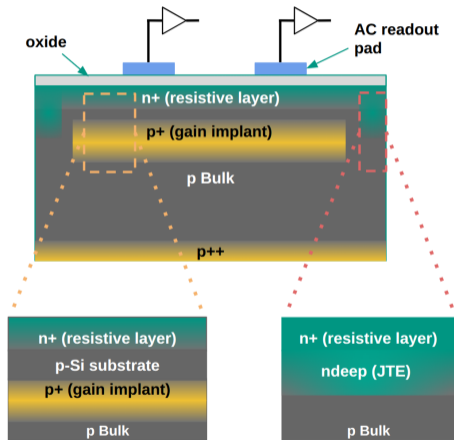
+



→



# Resistive Silicon Detector (RSD)

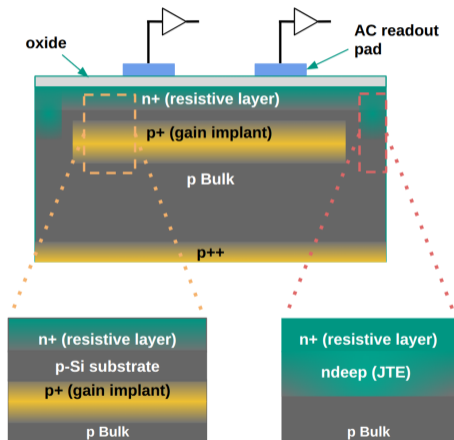


Reconstructing hit positions using the charge shared between **AC-pads**.

These sensors provide

- **precise spatial and temporal resolution,**
- an intrinsic 100% fill factor,
- a low density of readout channels.

# Resistive Silicon Detector (RSD)



Reconstructing hit positions using the charge shared between **AC-pads**.

These sensors provide

- **precise spatial and temporal resolution**,
- an intrinsic 100% fill factor,
- a low density of readout channels.

Many of its properties under **annealing** remain unstudied.

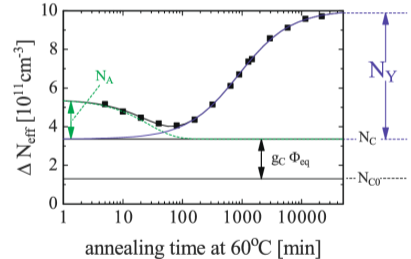
# Annealing: Hamburg Model

The Hamburg model, born to describe p-in-n sensors, parametrizes the space charge change due to donor removal plus acceptor creation with fluence and latter annealing.

Changing in effective donor doping concentration can be described by:

$$\Delta N_{\text{eff}}(\Phi_{\text{eq}}, t, T) = N_{C,0}(\Phi_{\text{eq}}) + N_A(\Phi_{\text{eq}}, t, T) + N_Y(\Phi_{\text{eq}}, t, T) \quad (1)$$

- $\Phi_{\text{eq}}$  stands for 1 MeV neutron equivalent fluence;
- Stable term  $N_{C,0}$ , most relevant in a high-radiation environment;
- The short-term annealing  $N_A$ , reducing the damage;
- The long-term annealing  $N_Y$ , degrading macroscopic sensor properties.



# Annealing: Hamburg Model

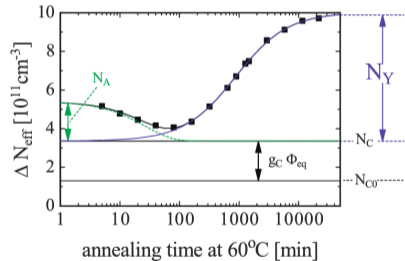
The Hamburg model, born to describe p-in-n sensors, parametrizes the space charge change due to donor removal plus acceptor creation with fluence and latter annealing.

Changing in effective donor doping concentration can be described by:

$$\Delta N_{eff}(\Phi_{eq}, t, T) = N_{C,0}(\Phi_{eq}) + N_A(\Phi_{eq}, t, T) + N_Y(\Phi_{eq}, t, T) \quad (1)$$

- $\Phi_{eq}$  stands for 1MeV neutron equivalent fluence;
- Stable term  $N_{C,0}$ , most relevant in a high-radiation environment;
- The short-term annealing  $N_A$ , reducing the damage;
- The long-term annealing  $N_Y$ , degrading macroscopic sensor properties.

1. Sensor bulk
2. Moderate doping



# Annealing: Hamburg Model

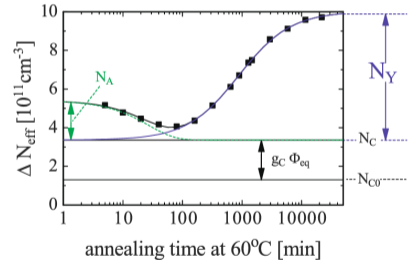
The Hamburg model, born to describe p-in-n sensors, parametrizes the space charge change due to donor removal plus acceptor creation with fluence and latter annealing.

Changing in effective donor doping concentration can be described by:

$$\Delta N_{\text{eff}}(\Phi_{\text{eq}}, t, T) = N_{C,0}(\Phi_{\text{eq}}) + N_A(\Phi_{\text{eq}}, t, T) + N_Y(\Phi_{\text{eq}}, t, T) \quad (1)$$

- $\Phi_{\text{eq}}$  stands for 1MeV neutron equivalent fluence;
- Stable term  $N_{C,0}$ , most relevant in a high-radiation environment;
- The short-term annealing  $N_A$ , reducing the damage;
- The long-term annealing  $N_Y$ , degrading macroscopic sensor properties.

1. ~~Sensor-bulk~~ → **Thin layer**
2. ~~Moderate doping~~ → **High doping concentration**



# Test Structure

Since our goal is to study the annealing in the resistive layer of the RSD, we used dedicated test structures. Van der Pauw structures are characterized by a cross-shaped geometry with four contacts placed at the edges of the layer under study.

The donor doping is monitored with sheet resistivity measurements.

There are two types of structures:

## n+

- Propagates the signal over the sensor.

→ **Arsenic doping**

## n deep

- JTE structure of the device.

→ **Phosphorus doping**

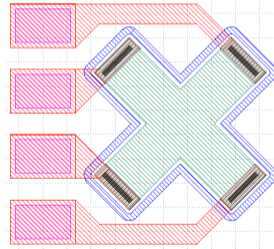


Figure: Sheet conductance in the n+ layer during the room temperature annealing.

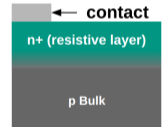


Figure: Van de Pauw cross section

# Doping concentration and Irradiation campaign

Different doping concentration:

$$n+: W_{low} < W_{medium} < W_{high}$$

$$n_{deep} : W_{medium}$$

Irradiation campaign at JSI TRIGA reactor and ZAG cyclotron located on the KIT campus.

neutron fluence [ $10^{15} \text{ cm}^{-2}$ ]	proton fluence [ $10^{15} \text{ cm}^{-2}$ ]
1.0	0.6
2.0	1.0
3.5	1.8
5.0	2.8



# Studies on Irradiated Test Structure

Perform four point **sheet resistance measurement** via the four contacts to monitor the **changes of the effective doping concentration**.

The voltage was measured while the input current was varied:

$n+$	-0.2 mA	to	0.2 mA	in step	$5 \mu A$
$n_{deep}$	-1.0 mA	to	1.0 mA	in step	$50 \mu A$

This sweeping method minimizes the influence of the contact resistance.

The sheet resistance was extracted by performing a fit of current versus voltage.

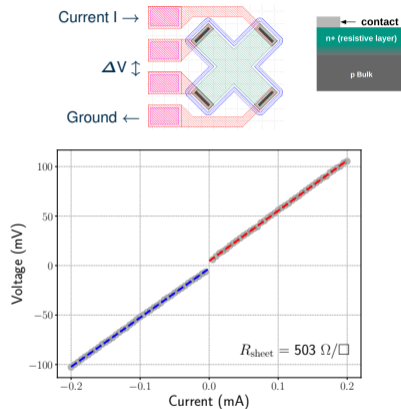


Figure: Sheet resistance measurement

# Isothermal Annealing in n+ and ndeep layer

- Sheet resistance of the test structure at regular intervals:
  - Hourly on the first day,
  - then daily,
  - and later every few days.
- For three temperature values, taken in subsequent intervals:
  - first days at room temperature (20 °C),
  - after 40 °C,
  - finally 60 °C.

# Isothermal Annealing in n+ and ndeep layer

- Sheet resistance of the test structure at regular intervals:
  - Hourly on the first day,
  - then daily,
  - and later every few days.
- For three temperature values, taken in subsequent intervals:
  - first days at room temperature (20°C),
  - after 40°C,
  - finally 60°C.

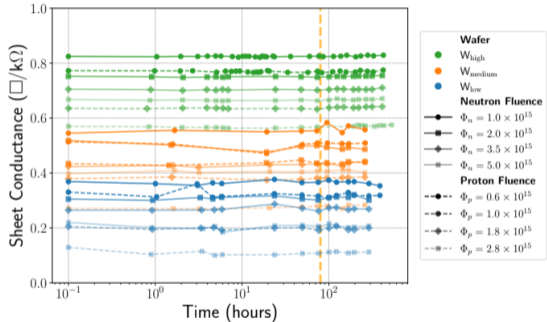
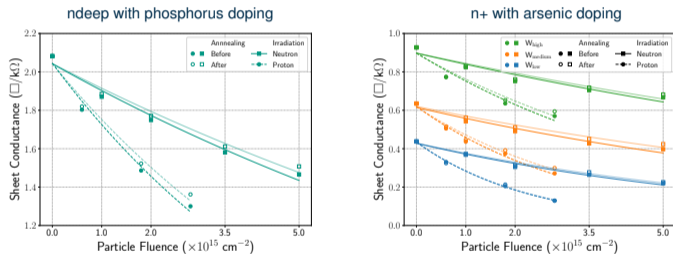


Figure: Sheet conductance in the n+ layer during first weeks room temperature annealing.

The **orange vertical line** refers to the approximate limit of beneficial annealing for the bulk in Hamburg Model.

# Isothermal Annealing in n+ and ndeep layer

The accumulated donor recovery can be monitored by observing the **effective donor removal** as a function of annealing.



$$f(\Phi) = Be^{-C_{eff}\Phi} \quad (2)$$

$\Phi$  is the fluence,  $f(\Phi)$  is the sheet conductance, and  $C_{eff}$  is the effective donor removal.

**Figure:** Fits to monitor the effective donor removal before and after the low temperature annealing campaign (20 + 40 + 60 °C).  $n_{deep}$  layer (left) and n+ layer (right).

# Isothermal Annealing in n+ and ndeep layer

The accumulated donor recovery can be monitored by observing the **effective donor removal** as a function of annealing.

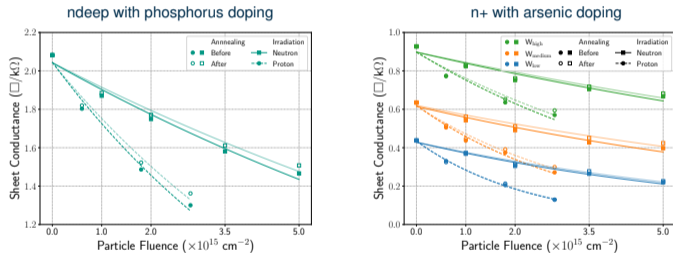


**Figure:** Fits to monitor the effective donor removal before and after the low temperature annealing campaign (20 + 40 + 60 °C).  $n_{deep}$  layer (left) and n+ layer (right).

$$f(\Phi) = Be^{-C_{eff}\Phi} \quad (2)$$

$\Phi$  is the fluence,  $f(\Phi)$  is the sheet conductance, and  $C_{eff}$  is the effective donor removal.

→ **Decreasing of sheet conductance with irradiation.**

→ **Small difference between before and after low-temperature annealing.**

# Isochronal annealing in n<sup>+</sup> and n<sub>deep</sub> layer

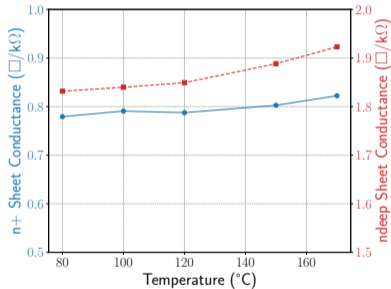
The defects have temperature dependence. ⇒ Increasing the temperature we can understand which defects are inside the sensor.

Investigate annealing at higher temperature.

- Steps of 20 minutes
- were used at temperatures of
- 80, 100, 120, 150, and 170°C.

# Isochronal annealing in n+ and ndeep layer

The defects have temperature dependence.  $\Rightarrow$  Increasing the temperature we can understand which defects are inside the sensor.



Investigate annealing at higher temperature.

- Steps of 20 minutes were used at temperatures of 80, 100, 120, 150, and 170°C.

Both the n+ and ndeep layers saw  $\approx$  5% increase in sheet conductance.

**Figure:** Sheet conductance during isochronal annealing in steps of 20 minutes. Both the n+ and ndeep layers are displayed (with different y-axes) for a  $W_{high}$  structure irradiated to  $2.8 \cdot 10^{15} \text{ cm}^{-2}$  with proton.

# 170°C Annealing in n+ and ndeep layer

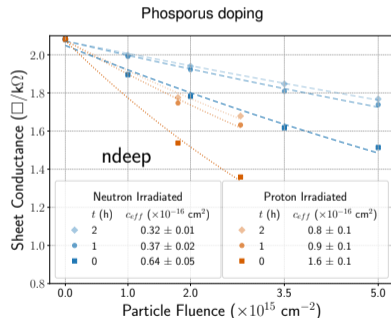
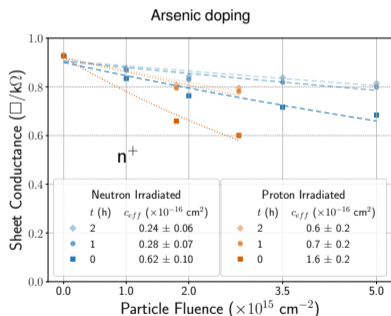
Above 150 °C it is possible to **break the defects** which trap phosphorus/arsenic in the interstitial position and potentially add **phosphorus/arsenic back to the lattice**, thus **recovering donor states**.

→ two isothermal steps of 1 hour at 170 °C

# 170°C Annealing in n<sup>+</sup> and n<sub>deep</sub> layer

Above 150 °C it is possible to **break the defects** which trap phosphorus/arsenic in the interstitial position and potentially add **phosphorus/arsenic back to the lattice**, thus **recovering donor states**.

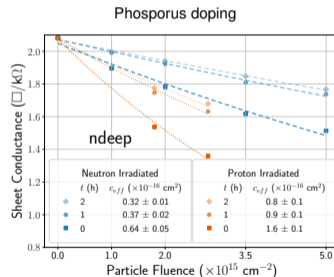
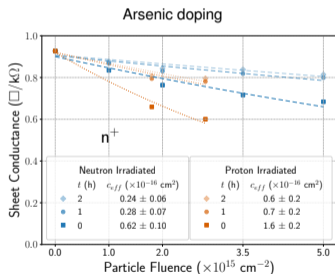
→ two isothermal steps of 1 hour at 170 °C



# 170°C Annealing in n<sup>+</sup> and ndeep layer

Above 150 °C it is possible to **break the defects** which trap phosphorus/arsenic in the interstitial position and potentially add **phosphorus/arsenic back to the lattice**, thus **recovering donor states**.

→ two isothermal steps of 1 hour at 170 °C



**The effective donor removal decreases considerably with the annealing at 170°C**

# Conclusions

The evolution of the effective doping concentration was investigated as a function of annealing and fluence.

- ✓ A small difference was observed between before and after low-temperature annealing (below 60 °C),  
⇒ High doped n+ layer will be stable during shutdown of experiment;
- ✓ High temperature isochronal annealing (70-150 °C) shows a  $\approx 5\%$  increase in sheet conductance for n+ and ndeep layers;
- ✓ Relevant donor recovery was observed with the annealing at 170 °C,  
⇒ In line with recombination of Arsenic-Silicon vacancy and Phosphorus-Silicon vacancy;

# Funding and Acknowledgments

- European Union's Horizon Europe Research and Innovation programme Grant Agreement No 101057511 (EURO-LABS)
- Alexander von Humboldt Stiftung
- INFN - Gruppo V RSD
- Dipartimenti di Eccellenza, Univ. of Torino (ex L. 232/2016, art. 1, cc. 314, 337)
- Ministero della Ricerca, Italia, PRIN 2017, progetto 2017L2XKTJ – 4DinSiDe
- RD50 Collaboration, CERN
- Hans Jurgen Simonis and Bernd Berger for technical help



# Backup

# How the PCBs change its temperature

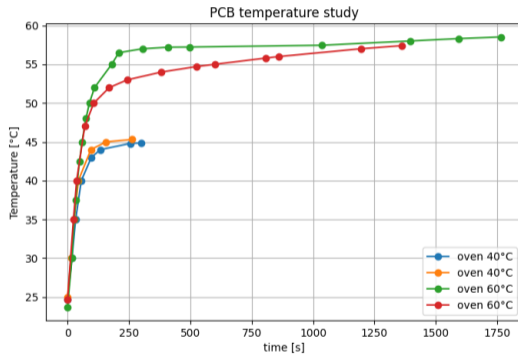
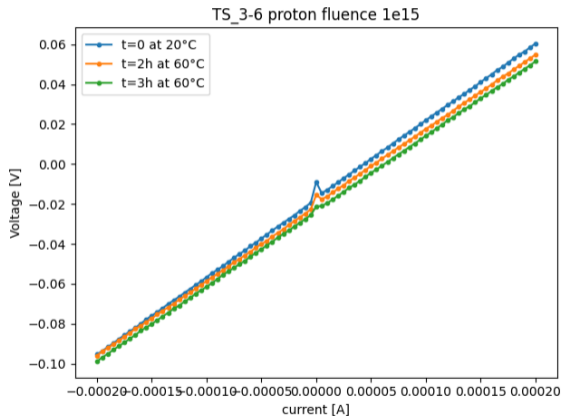


Figure: PCBs warm up into the oven

# Sheet resistance at 60°C



# Sheet conductance at 40°C and 60°C

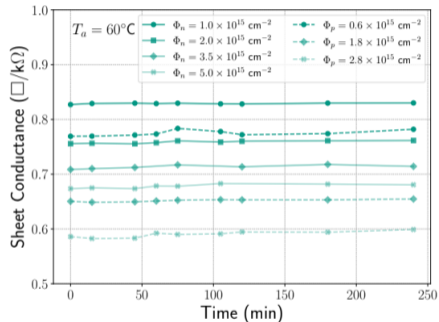
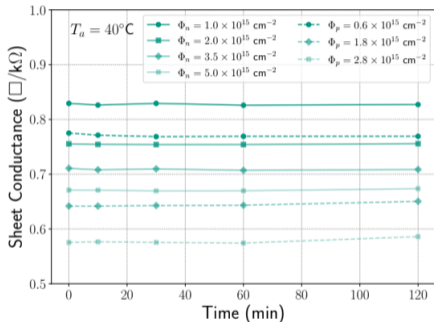


Figure: On left sheet conductance at 40°C. On the right measurements at 60°C

# Effective donor removal coefficient values

<i>c<sub>eff</sub></i> effective donor removal coefficient values [ $10^{-16}$ cm <sup>2</sup> ]					
Particle type	Annealing	W <sub>low</sub>	W <sub>medium</sub>	W <sub>high</sub>	W <sub>high</sub> ndeep
Neutron	Before	1.4 ± 0.1	1.0 ± 0.1	0.7 ± 0.1	2.6 ± 0.4
	After	1.3 ± 0.1	0.9 ± 0.1	0.6 ± 0.1	2.6 ± 0.4
Proton	Before	4.3 ± 0.1	3.0 ± 0.2	1.8 ± 0.3	4.8 ± 0.9
	After	4.2 ± 0.3	2.7 ± 0.2	1.6 ± 0.3	5.3 ± 0.8

Figure: Effective donor removal for low temperature annealing (below 60°C)

# Sheet conductance over time

